Sensitivity of paleoclimate simulation results to season definitions

Sylvie Joussaume, Pascale Braconnot

JOURNAL OF GEOPHYSICAL RESEARCH, VOL. 102, NO. D2, PAGES 1943–1956, JANUARY 27, 1997

Sensitivity of paleoclimate simulation results to season definitions

Sylvie Joussaume[1,2] and Pascale Braconnot[1]

Abstract. According to the Milankovitch theory, slow variations of the Earth's orbital parameters change the amplitude of the seasonal cycle of insolation and are considered to be the main forcing mechanism of glacial-interglacial cycles. Because of the precession and changes in eccentricity the length of seasons also varies. No absolute phasing is then possible between the insolation curves of two different periods. Various solutions to compare different periods have been given either for astronomical computations [e.g., *Berger and Loutre*, 1991; *Laskar et al.*, 1993] or for model simulations [e.g., *Kutzbach and Otto-Bliesner*, 1982; *Mitchell et al.*, 1988], but the sensitivity of model results to the different possible solutions has never been quantified. Our results, based on simulations of the last interglacial climate, 126 kyr B.P., where changes in the length of the seasons are large, clearly show that phase leads or lags between the various solutions used introduce biases in the analysis of insolation and climate change of the same order of magnitude as the Milankovitch forcing. Our main conclusions are that (1) when comparing various model simulations, the date of the vernal equinox (i.e., the phasing of the seasonal cycle of insolation) as well as the definition of seasons must be the same for all models in order to avoid artificial differences; (2) seasons based on astronomical positions are preferred to seasons defined with the same lengths as today, since they better account for the phasing of insolation curves. However, insolation is not the only forcing in most atmospheric general circulation model simulations. We also discuss the impact of the calendar hidden behind the definition of the seasonal cycle of the other boundary conditions, such as sea ice or sea surface temperatures.

1. Introduction

Slow variations of the Earth's orbital parameters modulate the insolation received at the top of the atmosphere [*Berger*, 1988]. Over periods of 100,000 and 400,000 years, eccentricity slowly varies from 0.0 to 0.0607, inducing small changes of the annual mean total insolation received by the Earth. Obliquity oscillates from 22° to 25° over a 41,000-year period and the position of the equinoxes precess relative to the perihelion with 19,000- and 23,000-year periods. Obliquity and precession do not lead to any change of the global annual mean energy received by the Earth but strongly modulate the seasonal pattern of insolation. Following the pioneering work of *Milankovitch* [1920], all these slow variations of insolation are considered to be the main driving process of the Quaternary glacial-interglacial cycles, although questions still remain to explain how this forcing and the observed climate changes are related [*Imbrie et al.*, 1992].

To investigate the impact of such changes of insolation on climate, atmospheric general circulation models (AGCMs) can be used. For example, sensitivity experiments have emphasized the impact of northern hemisphere (NH) summer insolation changes on the monsoon intensity during the mid-Holocene, 6 kyr and 9 kyr before present (B.P.) [*Kutzbach and Street-Perrot*, 1985; *Mitchell et al.*, 1988] as well as the processes leading to glacial inception at the end of the last interglacial when a strong decrease in NH summer insolation was experienced around 115 kyr B.P. [*Royer et al.*, 1984; *Rind et al.*, 1989; *Phillipps and Held*, 1994; *Gallimore and Kutzbach*, 1995]. An international modeling effort is also taking place within the Paleoclimate Modeling Intercomparison Project (PMIP) [*Joussaume and Taylor*, 1995] under the endorsement of the International Geosphere-Biosphere Program (Past Global Changes Core Project) and the World Climate Research Program (Working Group on Numerical Experimentation). About 17 models are being run under the same insolation changes for 6 kyr B.P. and compared, with the aim to study how much the simulated sensitivity to insolation depends on the parameterizations used and to better emphasize model capacities by comparison with available proxy data.

To perform simulations of past climatic periods, astronomical computations provide values of the orbital parameters [*Berger and Loutre*, 1991], and celestial mechanical laws allow to compute the daily incoming solar radiation [*Berger*, 1978]. To emphasize climatic changes, we also need to evaluate the differences of insolation and climatic variables between two different periods. However, because of the precession of equinoxes and the elliptical shape of the Earth's orbit the length of the seasons evolve through time; the number of days between equinoxes and solstices is indeed proportional to the area covered between the corresponding astronomical positions and can vary from 82.5 to 100 days over the last million years [*Berger and Loutre*, 1994].

To account for such a change in the length of the seasons, *Berger and Loutre* [1991] and *Laskar et al.* [1993] compare

[1]Laboratoire de Modélisation du Climat et de l'Environnement, CEA-DSM, Gif-sur-Yvette Cedex, France.
[2]Laboratoire d'Océanographie Dynamique et de Climatologie, CNRS, Université Pierre et Marie Curie, Orstom, Paris.

Paper number 96JD01989.
0148-0227/97/96JD-01989$09.00

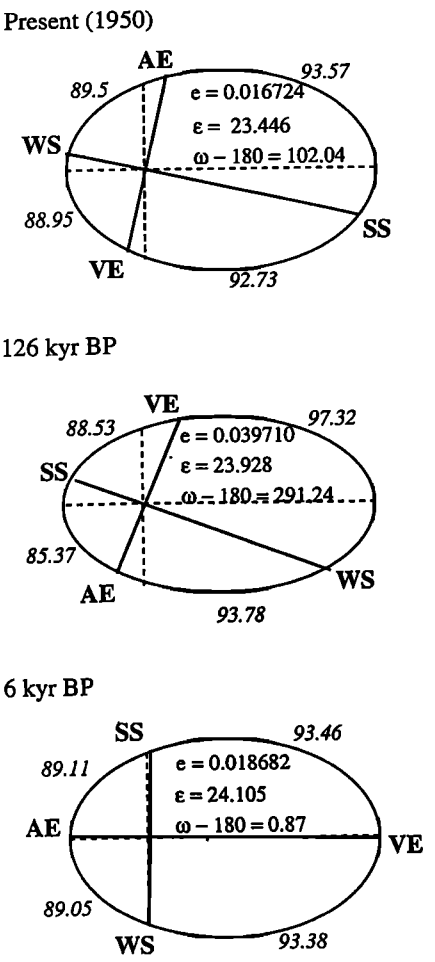

Figure 1. Earth's orbital elements for present, 126 kyr B.P., and 6 kyr B.P., where e is the eccentricity, ε is the obliquity, and ω is the longitude of the perihelion.

insolation values computed for the same astronomical positions, i.e., the same angular position, along the Earth's orbit relative to equinoxes and solstices. Indeed, comparing insolation curves for the same dates will be misleading. Even if we assign the same date to the vernal equinoxes of two different periods, then their autumnal equinox and solstices will automatically occur at a different date due to the change in the length of the seasons.

When considering paleoclimate simulations performed with an AGCM, different procedures have been followed. For example, for simulations of the 9 kyr B.P. climate, *Kutzbach and Otto-Bliesner* [1982] have accounted for the change in the length of the seasons, whereas *Mitchell et al.* [1988] have kept seasons similar to present day. These two simulations have also used a different reference date to define the "calendar" (i.e., assignment of a date to each day) at 9 kyr B.P.: *Kutzbach and Otto-Bliesner* [1982] have fixed the 9 kyr B.P. vernal equinox at March 21, and *Mitchell et al.* [1988] have fixed the 9 kyr B.P. summer solstice at June 22. Thus both the 9 kyr insolation changes and the 9 kyr B.P. minus present monthly mean differences cannot be directly compared between these two sets of simulations.

To date, no study of the impact of such choices of calendar and definition of seasons has ever been published. However, *Loutre* [1993] has shown significant differences when comparing insolation computed for two different periods either using the same astronomical portion or the same date. In the framework of PMIP, where model-model comparisons for past climate will be conducted, differences in the procedure used may not be negligible and need to be quantified.

In the following, we will discuss in details the influence of calendar and season definitions for paleoclimate simulations. To better emphasize the sensitivity to a change in the length of the seasons, we have essentially analyzed results for the 126 kyr B.P. climate for which the changes are more important than for the 6 kyr B.P. climate.

We first describe the orbital configuration for the period of interest. We then define two calendars to analyze the impact of the choice of a calendar on the solar radiation differences at the top of the atmosphere. Similar analyses are then conducted for the climate response, using simulations performed with the atmospheric general circulation model (AGCM) of the Laboratoire de Météorologie Dynamique (LMD).

2. Insolation Changes and Orbital Configuration

2.1. Defining a "Calendar" for Past Insolation

Today, Earth is at the aphelion during northern hemisphere (NH) summer, and at the perihelion during NH winter, whereas 126,000 years before present it was the contrary (Figure 1). The eccentricity was also higher at that time. Consequently, the NH summer season was shorter. Indeed, following the Kepler's laws, the time elapsed between two positions of the Earth along the ellipse is proportional to the area covered. If λ is the true longitude, i.e., the angle used to define the Earth position relative to the vernal equinox, then time and λ are related by

$$\frac{2\pi}{T}\,dt = \frac{r^2\,d\lambda}{a^2(1-e^2)^{1/2}}, \tag{1}$$

where r is the Earth-Sun distance, e is the eccentricity, T is the 1-year period, and a the semimajor axis of the elliptical orbit. For example, 126 kyr B.P., the precession of the equinoxes, together with a larger eccentricity, reduced the time between the vernal equinox (VE) and the summer solstice (SS) by 4 days, the time between SS and the autumnal equinox (AE) by 8 days but increased the time between AE and the winter solstice (WS) by 4 days and the time between WS and VE by 8 days (Figure 1). The differences were less 6 kyr B.P. but reached 4 days for the SS-AE and WS-VE intervals.

Equation (1) determines the Earth movement but does not provide any absolute reference for time along the orbit. To compare two insolation curves, like 126 kyr B.P. and today, we then need to phase one curve relative to the other in order to study the impact of changes in the seasonal variations of insolation. In other words, a reference date must be arbitrarily chosen if we want to define a past calendar, as is done for climate models.

The usual solution defines the date of the vernal equinox as the reference, i.e., fix March 21 at noon to VE for any period of the past. With this choice, two different insolation patterns are in phase around the vernal equinox but cannot be in phase around the autumnal equinox and the solstices (Figure 2) which thus occur at a different date for the two different past periods. However, there is no reason to prefer synchronized VE to any other position along the ellipse. In particular, the

date of AE (or of one of the solstices) could also be chosen as a reference. For instance, if we choose to phase the AE date for 126 kyr B.P. and today, we would end up with a curve similar to the previous one but shifted in time (Figure 2). These two curves describe the same insolation seasonal cycle, but compared to the present day for a given date, they lead to different changes in insolation. Around VE and AE, where the phase shift between the two 126 kyr B.P. curves is maximum (12 days), the difference represents about 10% of the insolation received and is as large as the difference between 126 kyr B.P. and present.

Differences induced just by different reference dates used for past calendars are, therefore, not negligible. Thus it is crucial for model-model comparisons to use exactly the same time reference (calendar) in all model simulations in order to compare the same daily insolation at the top of the atmosphere. For PMIP it was decided to fix the VE at March 21 noon.

2.2. Classical Versus Angular Definition of Seasons

Once a calendar has been defined for past climates, how do we account for the change in the length of the seasons to analyze model results? Two alternative procedures have been followed by modelers which are first compared for the insolation patterns and then for model results (section 3).

In most cases, once a reference date has been chosen, months or seasons are defined following the present-day calendar. In this procedure, referred to as "classical" in the following, averages are performed over the same number of days and for the same dates as today's, for any period of the past. However, following (1), months or seasons do not then cover the same portion of the Earth's orbit with respect to equinoxes and solstices for two different orbital configurations.

As an alternative definition of seasons, it seems appropriate to compare values of insolation for the same positions of the Earth along its orbit with respect to the VE [*Laskar et al.*, 1993]. Midmonths can be defined [*Berger*, 1978] by dividing the elliptical orbit in regular 30° increments of the true longitude, starting from the VE. Insolation patterns are then automatically phased for any period of the past since equinoxes and solstices are 90° apart from each other. Moreover, these patterns are independent of any time reference [*Suarez and Held*, 1979]. As a counterpart, these midmonths cannot be assigned the same calendar dates through time. Following this procedure, "angular" seasons can be defined, based on astronomy, as angular sectors along the orbit.

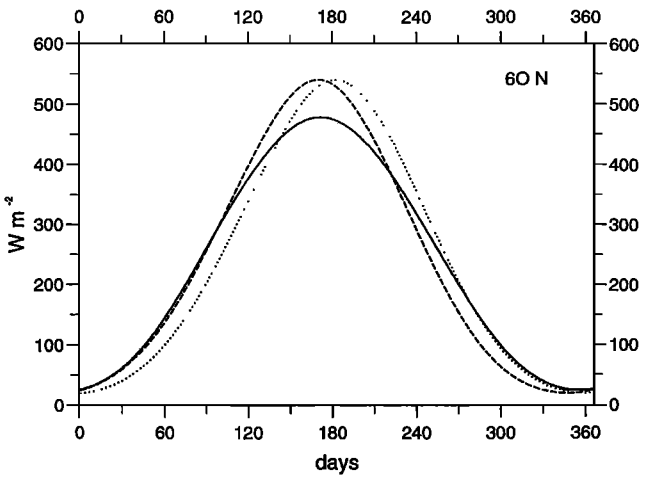

Figure 2. The 60°N daily insolation at the top of the atmosphere for present with March 21 as the vernal equinox (VE) date (solid line), 126 kyr B.P. with the same VE date as present (dashed line), and 126 kyr B.P. with the same autumnal equinox (AE) date as present, i.e., September 23 (dotted line). Solar radiation has been calculated with a solar constant So = 1365 W m^{-2} as recommended for the Paleoclimate Modeling Intercomparison Project (PMIP).

Table 1. First Day and Length of Angular Months for 126 kyr B.P. and 6 kyr B.P. (365-day Year) With Vernal Equinox Fixed to March 21

	126 kyr B.P.		6 kyr B.P.	
	Day/Month	Length	Day/Month	Length
January	25/12	34	28/12	32
February	28/01	31	29/01	30
March	28/02	32	28/02	32
April	01/04	30	01/04	31
May	01/05	29	02/05	31
June	30/05	27	02/06	29
July	26/06	28	01/07	30
August	24/07	28	31/07	29
September	21/08	28	29/08	29
October	18/09	32	27/09	30
November	20/10	32	27/10	30
December	21/11	34	26/11	32

The dates are referred to the present calendar months.

For today, the two approaches are equivalent. Our present-day Gregorian calendar, which is a lunisolar calendar, uses a temporal definition of months and seasons that follows the astronomical one. Indeed, if we define astronomical seasons as 90° sectors in longitude between equinoxes and solstices, modern NH winter seasons are shorter in time than modern NH summer seasons, since today the Earth's orbital speed is greater at perihelion than at aphelion. This is reflected in our calendar by 30 + 28 + 30 days in January-February-March against 31 + 31 + 30 in July-August-September.

In the following, we adopt an angular definition of months, similar to that of *Kutzbach and Gallimore* [1988], where "angular" months are defined by matching beginning and ending of celestial longitudes for each period. On the basis of these longitudes the number of days in each month and the dates relative to the present calendar months can be found using (1) and setting March 21 at VE (0° celestial longitude). Lengths and dates of "angular" months at 126 kyr B.P. and 6 kyr B.P. are given in Table 1 for a 365-day year.

2.3. Season Definition and Insolation Changes

Using the "classical" and the "angular" definitions of months defined above, we can display the insolation changes between 126 kyr B.P. and today as a function of both time and latitude (Figure 3).

Let us consider first Figure 3b where "classical" months are used and where we assume the same reference date for both the 126 kyr B.P. and the present VE (Figure 3a). As expected by the increase of eccentricity and the precession of the equinoxes, NH midlatitudes received about 40 to 50 W m^{-2} more energy during summer 126 kyr B.P. than today. The patterns of differences exhibit a large structure in autumn with a north-south orientation, indicating a solar radiation reduction of about 40 W m^{-2} 126 kyr ago at high northern latitudes in

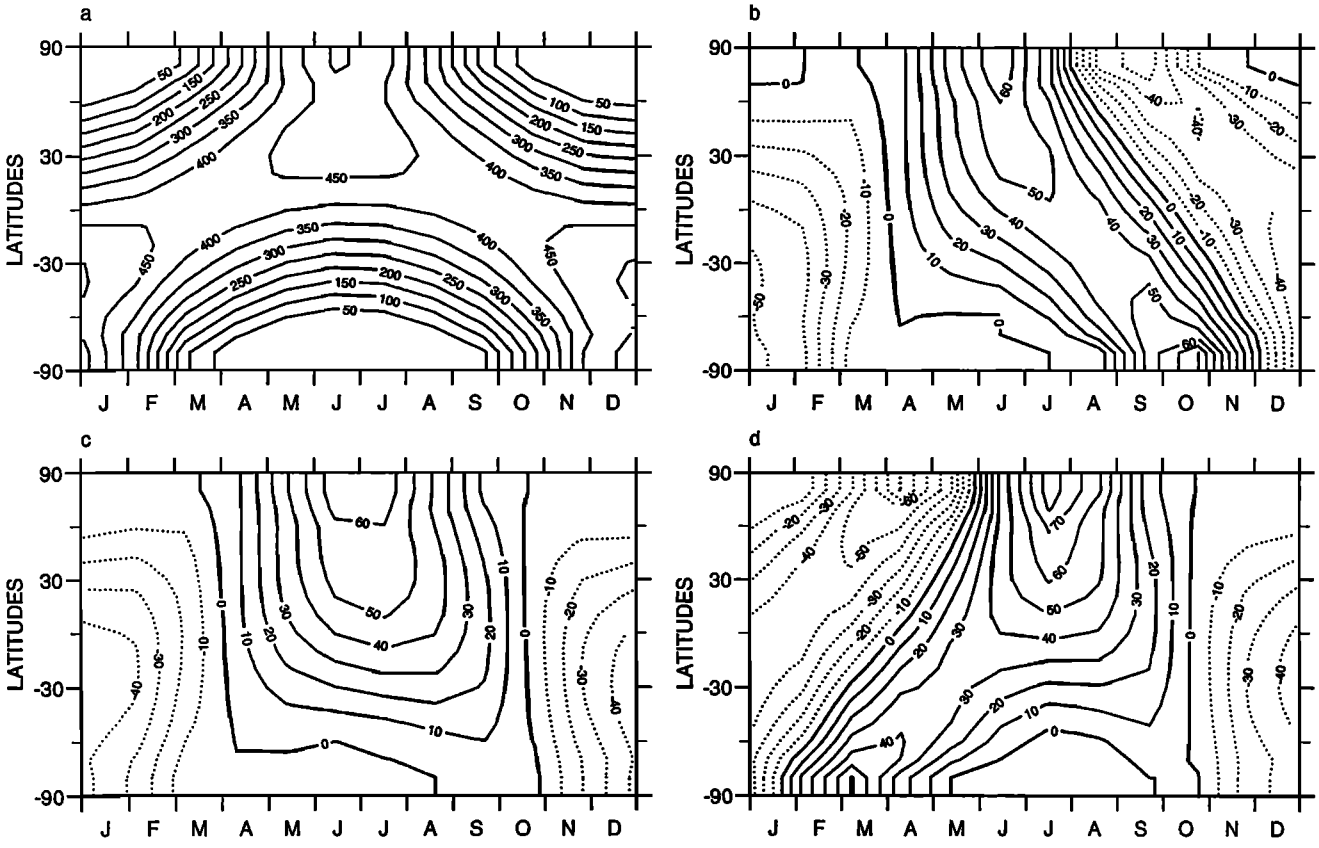

Figure 3. Monthly mean insolation (Wm^{-2}) at the top of the atmosphere as a function of latitude for (a) present, (b) 126 kyr B.P. minus present, with 126 kyr B.P. months based on classical means and the same VE date as present, (c) 126 kyr B.P. minus present, with 126 kyr B.P. months based on angular means, and (d) same as Figure 3b but with the same AE date as present.

September and an increase of about 60 W m^{-2} at high southern latitudes in October.

The "classical" definition of months being dependent on a reference date, we could have as well chosen to fix the autumnal equinox (AE) as a reference date (September 23 as for today). Although NH summers still receive more energy, the north-south orientation in autumn totally disappears and is replaced by a south-north orientation in spring (Figure 3d). These patterns are strongly dependent on the choice of time reference and simply reflect that 126 kyr ago the astronomical summer season was shorter. Indeed, when the date of the VE is imposed to be the same as today at 126 kyr B.P., the 126 kyr B.P. AE occurs on September 11. With this choice of reference date, the 126 kyr B.P. autumn begins earlier than today: insolation is consequently weaker in the NH and stronger in the SH, inducing a north-south pattern in Figure 3b. What is then called September at 126 kyr B.P. (September 1–30) is shifted by 12 days toward winter relative to the present-day orbital configuration, i.e., represents a mixture of present-day September and October with respect to the Sun declination. Similarly, the same analysis performed with a calendar reference date fixed at the AE leads to the conclusion that the 126 kyr B.P. spring began later (Figure 3d). The contradiction between the two figures (Figures 3b and 3d) then only results from an arbitrary choice of calendar, but there is no way to decide which one is right.

To avoid the arbitrary choice of reference date, let us consider the "angular" definition of months (Figure 3c). With this definition the large shifts found in autumn (Figure 3b) or spring (Figure 3d) totally disappear. Insolation values for the same astronomical positions are directly compared for two different climatic periods. No more phase lags or leads bias the insolation change patterns.

It is noteworthy that the differences between the "classical" or "angular" approaches, or even between two arbitrary choices of reference date for the "classical" months, can be as large as 40 W m^{-2}, i.e., as large as the Milankovitch forcing we are considering. As seen in the next section, this feature, also found for 6 kyr B.P. (not shown), just emphasizes that the Milankovitch forcing remains weak compared to the very strong seasonal variations of insolation.

2.4. Respective Impact of the Phase and Length of the "Monthly" Averages

However, none of the above ways to estimate monthly means is entirely satisfactory. With classical means, insolation patterns are not in phase and experience large differences according to the arbitrary calendar reference. Angular means seem more appropriate to analyze seasonal insolation differences, but the differences are performed between months that do not incorporate the same number of days. We can then wonder whether the change in the number of days introduced in the "angular" months does not produce a similar bias as the phase shifts associated with the classical means.

To answer this question and to emphasize which method is best, we compare the relative impact of a phase shift and of a

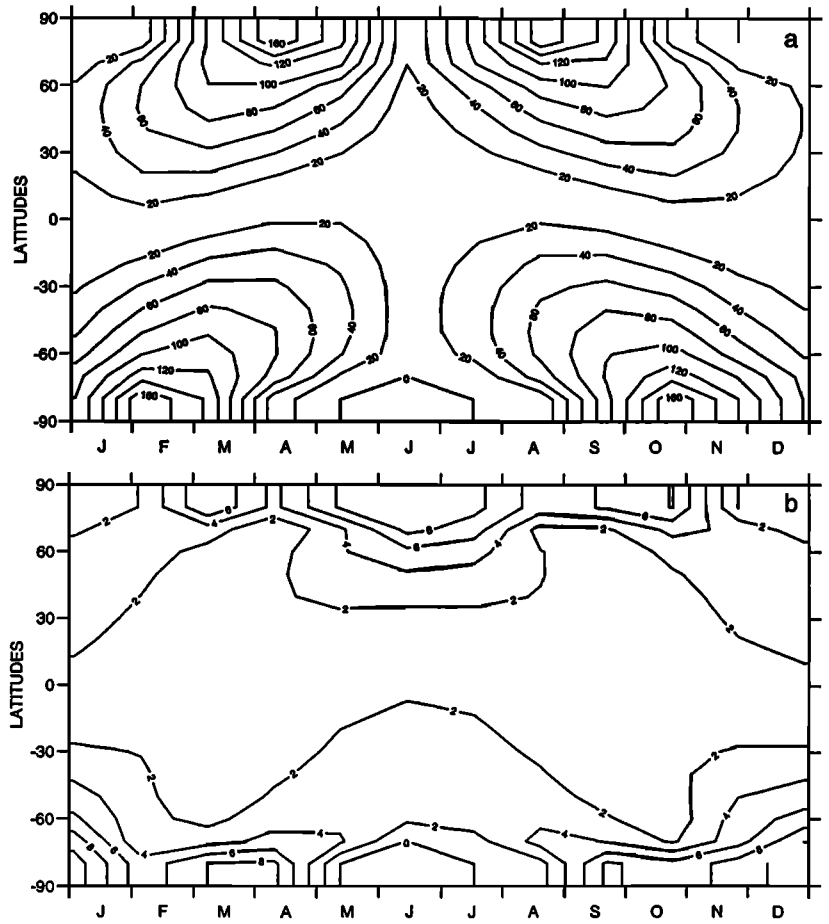

Figure 4. Mean root-mean-square errors (in 10^{-1} W m^{-2}) as defined in equation (3) in the estimation of monthly mean insolation as a function of time and latitude when (a) a phase shift ranging from −4 to +4 days is introduced for each month and (b) the length of the month is decreased or increased symmetrically from −4 to +4 days.

modification of the length of the months. We base our analyses on monthly average insolation computed for a present 365-day year.

To estimate the impact of a phase shift, we compute monthly mean insolations shifted by −4 to +4 days relative to the reference but including the same number of days. In that case, if N represents the number of days in the month, x_t the daily values of insolation, and δt the number of days by which the mean is shifted from the reference, the perturbed monthly mean for a given δt is

$$\bar{x}(\delta t) = \frac{1}{N} \sum_{t=\text{day}1+\delta t}^{\text{day}N+\delta t} x_t, \tag{2}$$

where day 1 and day N are the first and the last days, respectively, of a "classical" month. For δt varying between −4 and +4 days, the mean root-mean-square error is then

$$e = \text{sqrt}\left(\frac{1}{9}\sum_{j=1}^{9} (\bar{x}(\delta t_j) - \bar{x})^2\right), \tag{3}$$

with $\bar{x} = \bar{x}(0)$. Computed for each month and each latitude (Figure 4a), this error reaches 10 W m^{-2} in spring and autumn. This result is not surprising: for a phase shift δt, the difference between the perturbed mean and the reference can be approximated by

$$\Delta\bar{x}(\delta t) = \delta t \frac{(x_N - x_1)}{N} \tag{4}$$

which is of the order of the derivative of the insolation curve. The error is thus maximum at high latitudes where the amplitude of the seasonal cycle is the largest and for months near the equinoxes. The derivative can reach 90 W m^{-2} over 1 month. For a 4-day shift in insolation it leads to an error of 12 W m^{-2}. For 126 kyr B.P., where the shift reaches 12 days, we obtain about 36 W m^{-2}. The phase shift alone can then explain most of the features displayed in Figures 3b (3d) in autumn (spring).

Similarly, we can estimate the impact resulting from a change in the length of months by considering the mean root-mean-square differences between monthly means computed with more or less days than the reference but in phase with the reference (days are added or subtracted symmetrically). In that case, for a given δt the perturbed monthly mean is

$$\bar{x}(\delta t) = \frac{1}{(N + 2\delta t)} \sum_{t=\text{day}1-\delta t}^{\text{day}N+\delta t} x_t \tag{5}$$

and the mean root-mean-square error for δt varying from -4 to $+4$ days is also given by (3). This error (Figure 4b) is of the order of 1 to 2 W m^{-2} at high latitudes and is smaller than the previous ones by an order of magnitude. In that case, the difference between the perturbed mean and the reference can be approximated by

$$\Delta\bar{x}(\delta t) = \frac{2\delta t}{N + 2\delta t}\left(\frac{x_N + x_1}{2} - \bar{x}\right) \quad (6)$$

which is small since $(x_N + x_1)/2$ practically equals $\bar{x}$ in most cases, except at high latitudes near solstices. Variations of a few days in the length of a month have nearly no impact on the monthly mean.

The error done on angular means is thus a second-order effect compared to the error introduced on classical means by phase shifts. Angular means then seem more appropriate to study insolation differences between two climates, at least when looking at differences induced by changes in orbital parameters.

3. Implications for Model Results

3.1. Numerical Experiments

The way monthly means are defined is very sensitive when analyzing insolation changes. We may wonder how much it may influence the analyses of model results. In the following, we study the impact of monthly mean definitions on the comparison between 126 kyr B.P. and modern climates, as simulated by the AGCM developed at the Laboratoire de Metéorologie Dynamique (LMD) [*Sadourny and Laval*, 1984; *Le Treut and Laval*, 1984].

Simulations have been performed with version 4 of the LMD model [*Le Treut and Li*, 1991], using the low-resolution version which includes 48 grid points regularly spaced in longitude, 36 points regularly spaced in sine of latitude, and 11 vertical levels. The model includes the radiative scheme described by *Fouquart and Bonnel* [1980] for solar radiation and the scheme developed by *Morcrette* [1991] for infrared radiation. Condensation is produced using three schemes in a sequential mode: a moist adiabatic adjustment [*Manabe and Strickler*, 1964], a Kuo-type scheme [*Kuo*, 1965], and supersaturation for nonconvective precipitation. In this version of the model the land surface scheme is quite simple [*Laval et al.*, 1981] and computes soil moisture for a single 1-m-deep soil layer. Surface albedo is prescribed from climatology [*Schutz and Gates*, 1972] but is increased whenever there is snow. The model is used with full seasonal cycle but no diurnal cycle.

In the two experiments the CO_2 level has been fixed to preindustrial value (270 ppm), sea surface temperatures (SST) and both sea ice temperatures and sea ice extent have been prescribed to their modern values. The experiments only differ by their orbital parameters, which are given in Figure 1. For both climatic periods we keep March 21 at noon as the VE reference date. The model is run with a 360-day year which does not change the conclusions obtained in section 2. Each simulation is a 16-year run. The mean seasonal cycle is estimated by averaging the last 15 years, and the departures from the mean seasonal cycle for each of the 15 years are used to estimate the model internal variability and assess the statistical significance of the results.

A full discussion of the simulations can be found in *de Noblet et al.* [1996]. We therefore only recall here the main features

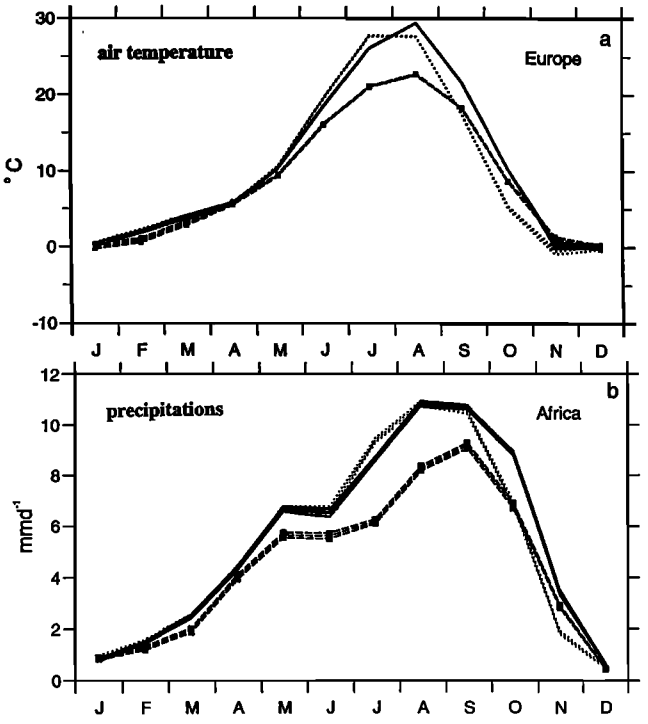

Figure 5. (a) Simulated surface air temperature over Europe and (b) precipitation over Africa for present (dashed line), 126 kyr B.P. using classical monthly means (dotted line), and 126 kyr B.P. using angular monthly means (solid line). Europe corresponds to all the continental grid points from 40°N to 70°N and 10°W to 30°E. Central Africa is the region extending from 6°N to 20°N and 13°W to 45°E. Error bars represent the 95% confident interval for the mean accounting for the interannual variability.

characterizing the 126 kyr B.P. climate. In response to the increased northern hemisphere seasonality of insolation at 126 kyr B.P., surface air temperature was 3° to 7°C warmer over most of Eurasia. The land/sea contrast was therefore enhanced, and the monsoon flow penetrated farther inland. Precipitation was increased over northern India, southern Tibet, and western China, exceeding present-day values by 4 to 5 mm d^{-1}, and was decreased over the southern tips of India, Indochina, and in southeastern Asia. A similar intensification was simulated in equatorial Africa with increased precipitation over the Sahel and southern Sahara.

3.2. Discussion of Model Results

In this paper, we only focus on the impact of season definition on the analyses of the differences between the two climates. We have thus performed the monthly means at 126 kyr B.P. using the classical and the angular definition of months, as defined in section 2 (for a 360-day year, see appendix). Following these definitions, monthly averages of surface air temperature over Europe (10°W–30°E; 40°N–70°N) and of precipitation over central Africa (13°W–45°E; 6°N–20°N) are plotted as a function of month in Figure 5 for 126 kyr B.P., and are compared to the present-day results. The error bars represent the 95% confidence interval accounting for the model interannual variability. Note that when classical monthly means are used at 126 kyr B.P., the months in Figure 5 have the same calendar dates as today but not the same longitudes along the

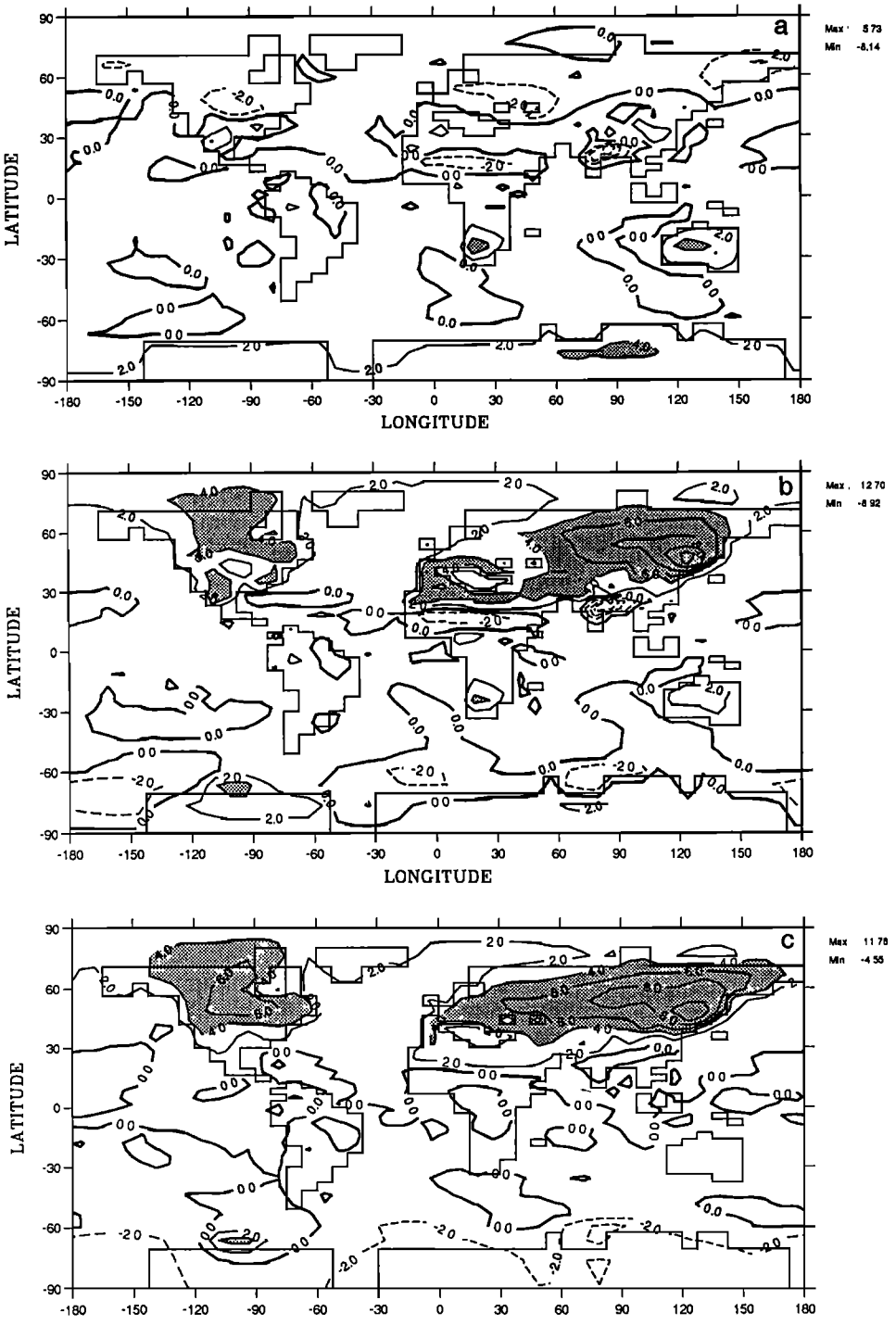

Figure 6. September air temperature differences between (a) 126 kyr B.P. classical means and present, (b) 126 kyr B.P. angular means and present, and (c) 126 kyr B.P. angular means and 126 kyr B.P. classical means. Isolines at every 2°C.

Earth's orbit relative to equinoxes and solstices. On the other hand, when angular monthly means are considered on the same figure, the 126 kyr B.P. months have the same longitudes relative to equinoxes and solstices as today but not the same calendar dates. Thus the two 126 kyr B.P. curves describe the evolution of surface air temperature and precipitation as a function of the period in the year rather than as a strict function of time.

For both definitions of monthly means, similar features are observed. Changes in the orbital parameters at 126 kyr B.P. produce large climatic changes, with a temperature increase of about 5°C over Europe in summer and about 6 mm d^{-1} more precipitation over Africa. However, as for the insolation patterns (Figure 3), the major differences between the two season definitions are displayed in autumn. As can be inferred from the error bars, they are statistically significant and even as large as the differences between 126 kyr B.P. and present. This is due to a combined effect of choosing the VE as a reference date

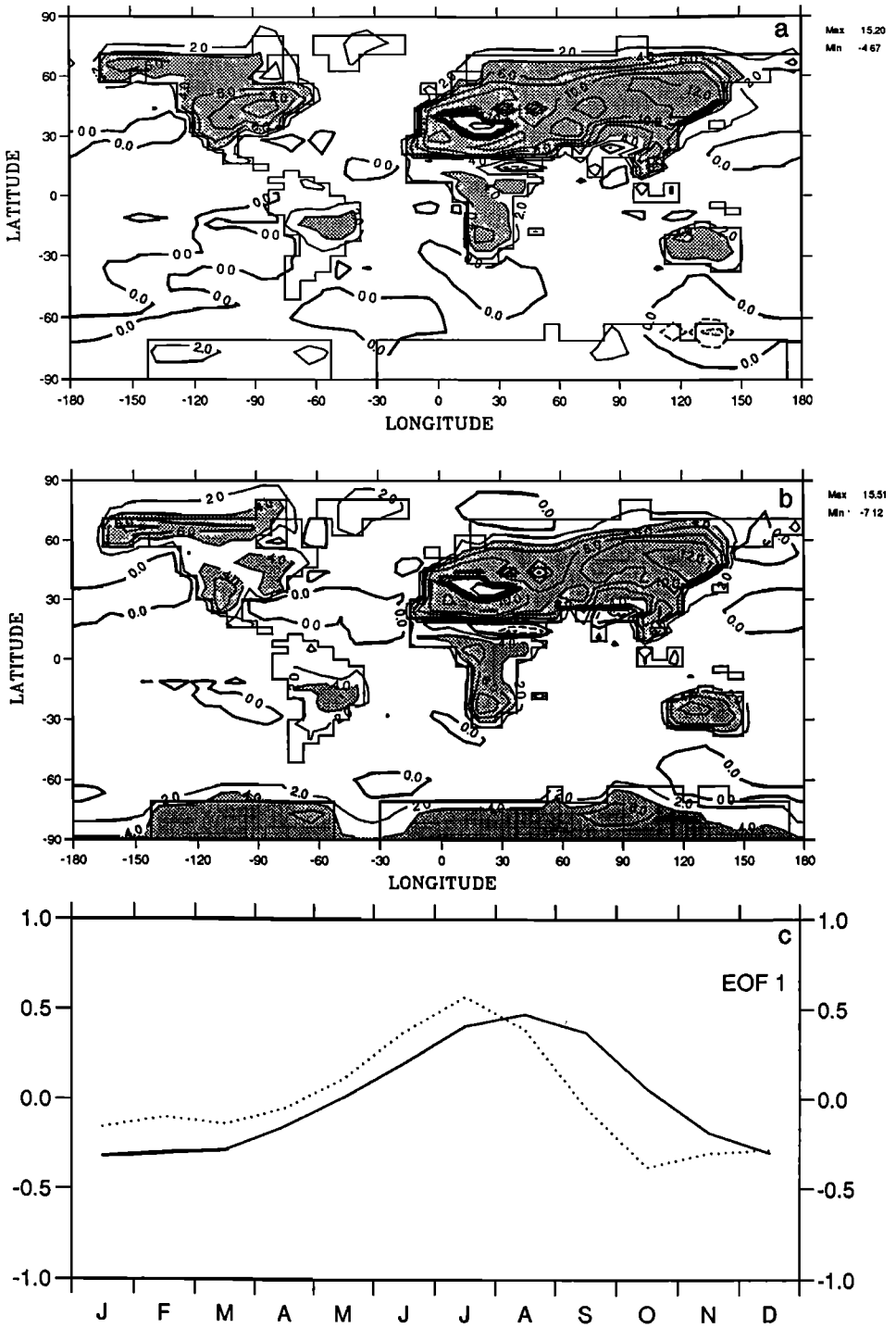

Figure 7. First component of the empirical orthogonal function (EOF) analysis of the surface air temperature difference between 126 kyr B.P. and present. Principal component of the difference (in relative units) with (a) 126 kyr B.P. classical monthly means and (b) 126 kyr B.P. angular monthly means. (c) Basic vector of the difference with 126 kyr B.P. monthly means defined as classical means (dotted line) and 126 kyr monthly means defined as angular means (solid line).

and of a shorter summer season at 126 kyr B.P. With our definitions, 126 kyr B.P. seasonal curve using classical mean leads the present one in autumn by about 13 days. Therefore the climatic variable autumnal averages at 126 kyr B.P. are biased toward the NH winter season: temperatures are already colder over Europe (Figure 5a) and precipitation weaker over Africa (Figure 5b). With any other time reference chosen along the orbit, the 126 kyr B.P. classical mean curve would just be shifted relative to the control experiment, and phase leads or lags would occur somewhere else in the year. On the other hand, the 126 kyr B.P. angular mean curve and the present one are in phase relative to insolation, and in autumn the 126 kyr B.P. temperatures are still warmer than today over Europe, and precipitation is still enhanced over Africa. Using angular

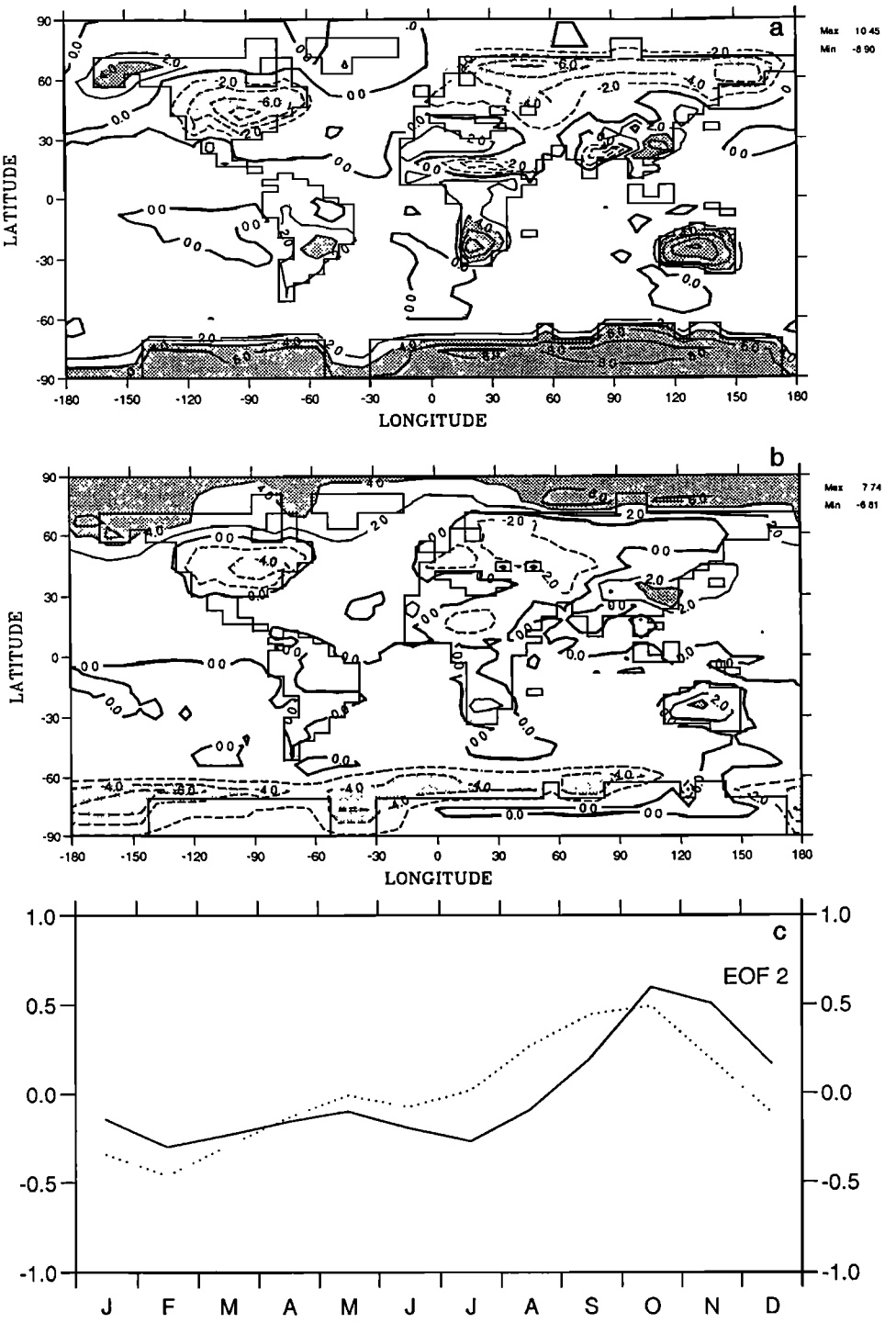

Figure 8. Same as Figure 7 for the second EOF.

means emphasizes changes that occur within seasons defined by the solar forcing, regardless of any reference date, such as the VE.

Such differences between the two methods are not just local. For example, let us consider September (Figure 6) when the differences between the two ways of analyzing the results are maximum due to the phasing of the VE. The surface air temperature differences displayed over Europe (Figure 5) extend over much of the NH continents (Figure 6c). They reach a maximum over eastern Asia and North America, with more than 10°C (Figure 6c), largely exceeding the differences between 126 kyr B.P. and today. Differences in these two areas are larger than the model internal variability and are statistically significant, as confirmed by a student t test (not shown).

3.3. Space and Time Patterns Associated With Each Season Definition

To better emphasize how the seasonal cycle is affected by the changes in insolation, we have computed the empirical orthog-

onal functions (EOFs) of the differences of surface air temperature between the 126 kyr B.P. seasonal cycle and the present one. EOFs have been computed for both definition of months for 126 kyr B.P.: the classical definition of months (Figures 7a and 8a), or the angular definition of months (Figures 7b and 8b). Time series are normalized and represent the basic vectors (Figures 7c and 8c); spatial fields are the empirical functions (in relative units). EOFs obtained with the two definitions of monthly means for 126 kyr P.B. are superimposed over the same figure to better contrast the results.

The first EOF (Figure 7) accounts for nearly the same amount of total variance for the two methods, with 58% and 60% for the classical and angular means, respectively. Their spatial fields are roughly similar and both exhibit the same warming pattern over most areas at 126 kyr B.P., except over Antarctica. Considering the temporal signal (Figure 7c), these warming patterns mainly correspond to an increased seasonal contrast in the NH and a decreased one in the SH, as expected from the precessional effect. Figure 7c also exhibits a strong phase shift in time. As already seen on Figure 5, the classical and angular means strongly differ in autumn.

The second EOF still accounts for a large amount of the total variance, 23% for 126 kyr B.P. using classical means minus present and 15% for the 126 kyr B.P. angular means minus present. However, both the EOF and the principal component differ (Figure 8). For classical means, a positive peak occurs in autumn when the first EOF reverses sign (Figure 8c). It corresponds to a cooling over the NH continents and a warming over Antarctica (Figure 8a). This pattern follows the strong negative/positive pattern exhibited from north to south for insolation arising from phase shifts due to a reduced length of the NH summer season and the particular choice of VE reference date (Figure 3b). Therefore as much as one fourth of the signal seems to be needed to represent a phase shift resulting from an arbitrary choice of calendar reference.

Since angular means do not introduce such a bias, the second component of the seasonal change, when 126 kyr B.P. cycle is computed using angular means, exhibits a very different pattern (Figure 8b). It emphasizes a response of high latitudes with a positive peak in late autumn (Figure 8c). Such a pattern corresponds to warmer surface air temperatures over the Arctic sea ice and colder ones over Antarctic sea ice in October-November. However, most of this feature is attributable to the calendar hidden under our surface boundary conditions, as is discussed in section 4.

4. Constraint Associated With Surface Boundary Conditions

4.1. Surface Boundary Conditions and Calendar

Indeed, an atmospheric model is not only forced by solar radiation incoming at the top of the atmosphere but also by prescribed surface boundary conditions such as SST. In our simulations the seasonal cycle of SST at 126 kyr B.P. has been fixed following the present-day cycle, keeping track of the present-day calendar in the 126 kyr B.P. simulations. With respect to boundary conditions, "classical" months appear then to be more appropriate than "angular" months. Indeed, when calculating angular means, we introduce an artificial phase shift between 126 kyr B.P. and modern surface boundary conditions. However, the seasonal cycle of SST has a relatively weak amplitude, due to the high ocean thermal capacity, and differences in SST monthly means computed using either the classical or the angular definition of months do not exceed 1°C (see Figure 9 for June and September).

In the simulations described in section 3, this constraint was particularly strong. We have performed the simulations with a version of the LMD AGCM that prescribes not only SST but also sea ice temperature. The seasonal cycle of sea ice temperature is much stronger than for SST and is therefore more sensitive to the definition of months. In June, differences reach 4°C in a few places around Antarctica, when the angular mean is slightly biased toward NH winter (Table 1). The maximum differences occur in September when the phase shift is largest. For that month, differences are negative in the southern hemisphere and positive in the northern hemisphere, since angular means are shifted toward NH summer. Such features are similar to the patterns found in high latitudes for the second EOF of angular means (Figure 8b). Figure 9 clearly shows that the calendar hidden under our boundary conditions bias the use of angular means.

4.2. New Set of Experiments

In order to determine which amount of the second EOF variance is to be attributed to the inconsistency between the astronomical seasons and the calendar hidden behind our boundary conditions, we have performed a new set of experiments, a control and a 126 kyr B.P. simulation, using a modified version of the LMD model. This version differs from the previous one (section 3) by including a simple model of sea ice. Sea ice extent is prescribed, but a prognostic equation has been introduced for the sea ice temperature, accounting for the surface energy fluxes exchanged with the atmosphere and heat conduction through a 3-m-thick ice core. Except at high latitudes over sea ice, the main features of the 126 kyr B.P. climate are very similar to the one presented in section 3. This allows us to conclude that the bias associated with the prescribed temperature over sea ice remains small. EOFs have also been applied to the new set of simulations for both definitions of months.

For the 126 kyr B.P. classical means, similar results to Figure 7a and 8a are obtained (not shown), with respective variances of 52% and 27% for the first and second components. For the 126 kyr angular means, however, the first EOF remains similar to Figure 7b (not shown), but the large latitudinal structures previously found at high latitudes for the second EOF (Figure 8b) completely disappear (Figure 10). This result confirms how much our previous angular mean analyses were biased by the sea ice temperature calendar (Figure 8b). The first EOF now represents 69% of the total variance and the second one is reduced to only 9%, being difficult to distinguish from the third one (7%). It is now clear that angular means better capture the main changes of the seasonal cycle due to insolation changes. By using two versions of the LMD model we were also able to emphasize the importance of the calendar associated to boundary conditions.

We may argue that a hidden calendar still remains behind our fixed daily sea surface temperatures. To account for the change in the length of the seasons, one possible solution could be to redo a daily interpolation of SSTs by assigning the present-day monthly means to the 126 kyr B.P. angular monthly means, i.e., by performing an interpolation accounting for the modified lengths of months. However, the remainder bias on the SST seasonal cycle at 126 kyr B.P. is an order of magnitude smaller than the one we had on sea ice tempera-

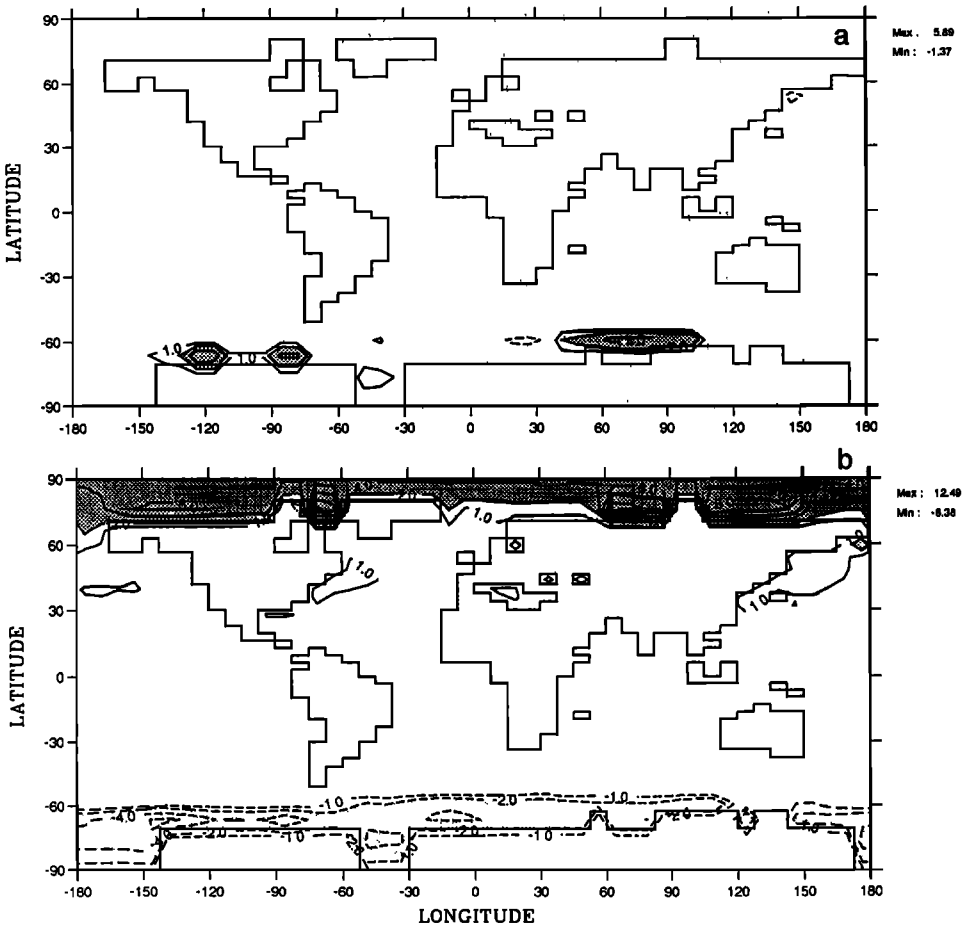

Figure 9. Differences of the monthly mean prescribed surface temperatures (sea ice and sea surface temperature) between the 126 kyr B.P. angular months and the present months for (a) June and (b) September. Isolines at every 1°C.

tures (Figure 9). Moreover, this procedure would never ensure that the resulting modified seasonal cycle would be entirely consistent with the simulated period. The only way to avoid such biases in the boundary conditions is to use a slab ocean, or a coupled atmosphere-ocean model, which calculates its own SSTs as a function of the surface energy budget. In this case, no more hidden calendar remains and angular means seem even more appropriate to account for insolation changes.

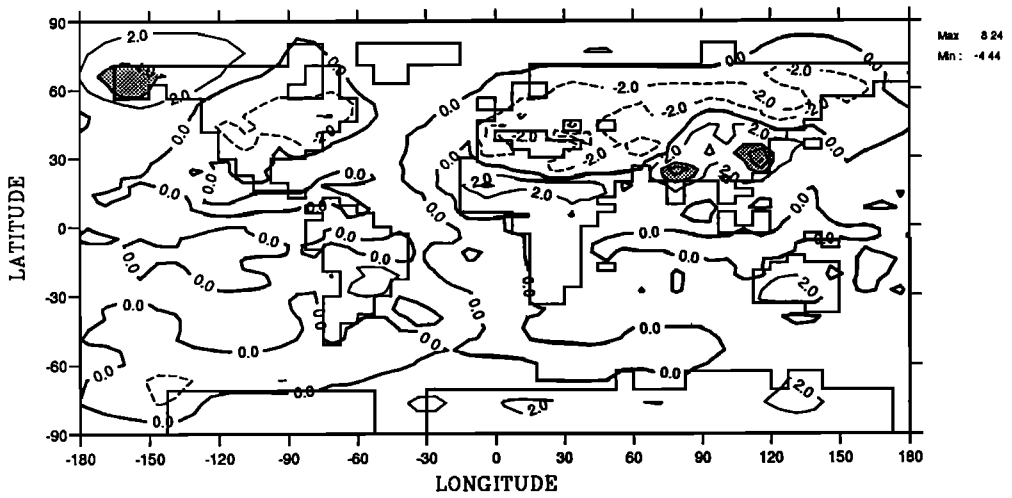

Figure 10. Second EOF of the difference of surface air temperature between the 126 kyr B.P. angular monthly means and the present ones for the second set of simulations using a modified version of the Laboratoire de Meteorologie Dynamique atmospheric general circulation model, including a simple sea ice model.

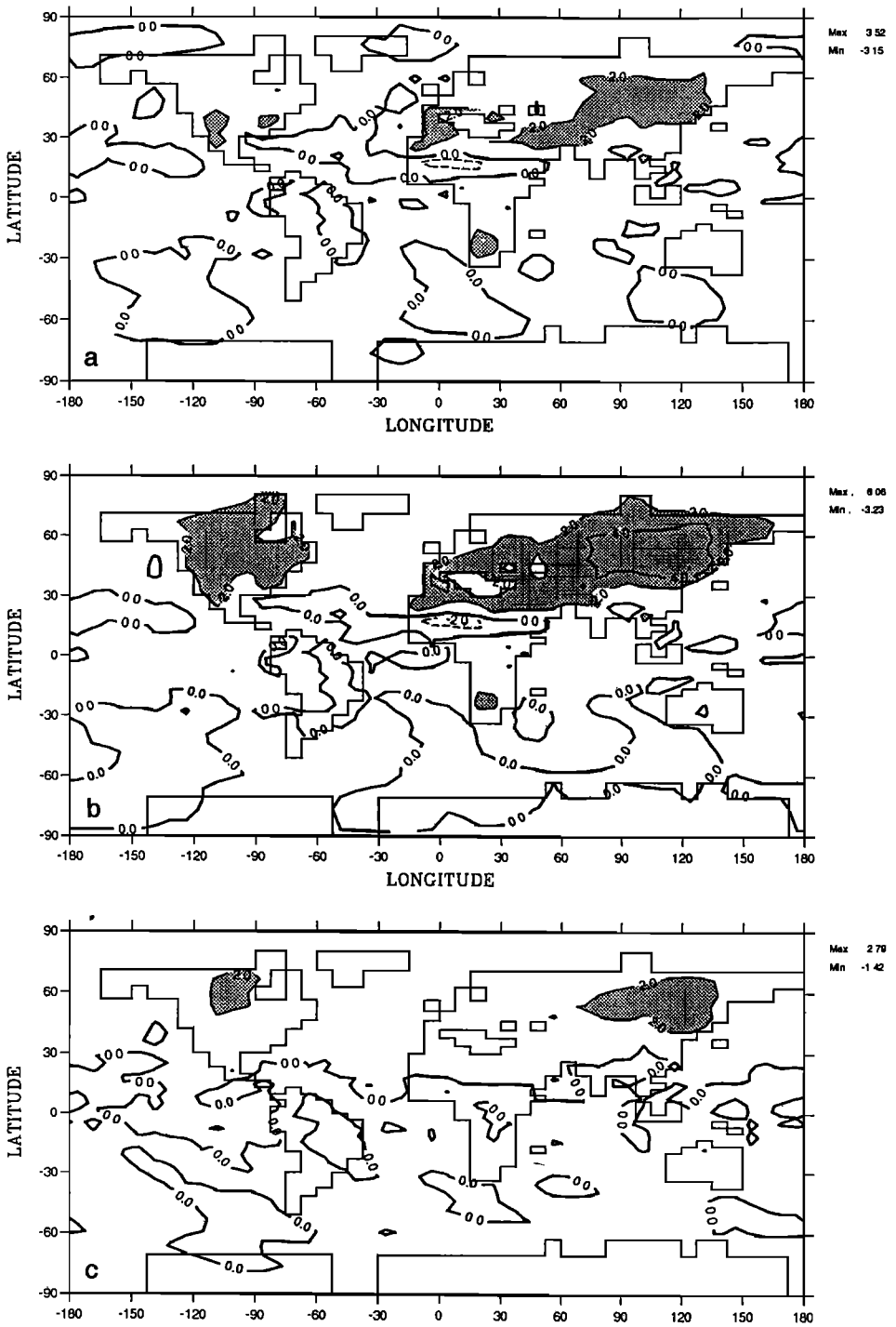

Figure 11. September surface air temperature differences between (a) 6 kyr B.P. with classical means and present, (b) 6 kyr B.P. with angular means and present, and (c) 6 kyr B.P. with angular means and 6 kyr B.P. with classical means. Isolines at every 2°C.

5. Conclusions

When modeling past climates, we need to address the question of defining a calendar for past periods. Indeed, because of precessional effects amplified by eccentricity changes, the length of seasons evolves through time. At least, when comparing two model simulations for past climates, the same reference date must be used in order to avoid biases in the phase relationship between the two model simulations.

Such biases may also be introduced artificially when comparing model results for two different climatic periods. In that case, no absolute phasing is possible due to changes in the length of the seasons. Any choice of calendar, or reference date to phase the two insolation curves, is arbitrary, and classical means arbitrarily depend on this reference date. The only way to avoid biases in the analyses due to phase lags or leads in the seasonal cycle is to introduce seasonal analyses based on

astronomical positions or angular positions along the elliptical orbits. Such a definition of seasons is physically based and allows to better analyze the response of climate to changes in insolation forcing. As demonstrated here, the use of one or the other approach has implications on the quantification of the changes between two periods. The main changes in the seasonal cycle appear in both season definitions, "classical" or "angular," but differences can appear for some seasons that may bias and even change the interpretation of model results.

Although already stated by several authors, differences between the various possible procedures had, until now, not been quantified. Our analyses show that such differences cannot be neglected. It also suggests that when reporting paleoclimate simulation results, it is necessary to specify not only the calendar reference but also which definition of months has been chosen for model analyses. Similar conclusion were also obtained for 6 kyr B.P. experiments, as illustrated in Figure 11 from changes in September surface air temperatures. However, the amplitude is weaker because the changes in the length of the seasons at 6 kyr B.P. lead at most to a shift of 5 days compared with the present.

Using months based on astronomical longitudes may also be of interest for the present-day orbital configuration when comparing models using a 365-day year and models using a 360-day year. Indeed, the same type of problem arises when we want to define a calendar for a 360-day year simulation. With the LMD model used in this paper, the VE date is fixed at March 21 and 30-day-long months are then defined. Such months then cannot keep the same phase for insolation relative to monthly means based on a 365-day year. Differences between the two insolation curves (not shown) can reach 5 to 8 W m^{-2} at high latitudes, as a result of shifts of a few days. Such biases were already discussed by *Slingo* [1982] who shifted the 360-day year date of the perihelion by 1 day to minimize the differences with a 365-day year. Using angular means for the 360-day year, i.e., defined on the same longitude values as for the 365-day year, completely erase such differences.

However, using angular or classical seasons does not solve all the questions addressed by model analyses. Some phenomenon may require more detailed analyses through time series, such as the 30- to 60-day oscillation. Statistical analyses of temporal series would have to be done separately for the two climatic periods. Both the impossibility to phase two insolation curves and the chaotic nature of the atmospheric circulation would cancel the possibility to produce day-by-day differences.

We have shown a strong sensitivity of the changes of climatic variables according to the procedure used to define seasonal or monthly means. We may then wonder which procedure is more adequate to compare model results to proxy data. The choice may depend on the type of proxy data. Our feeling is that in most cases, plants or living species will be sensitive to the seasonal cycle of insolation, i.e., astronomical positions, in agreement with the use of angular months. However, we would like to leave this question open for discussion among paleoclimatologists.

Appendix: Angular Means for a 360-day Year

The LMD model uses a 360-day year. Then, angular monthly means are defined in Table A1 as follows:

Table A1. First Day and Length of Angular Month for 126 kyr B.P. and 6 kyr B.P. for a 360-day Year

	126 kyr B.P.		6 kyr B.P.	
	Day/Month	Length	Day/Month	Length
January	24/12	33	27/12	31
February	27/01	33	28/01	32
March	30/02	31	30/02	31
April	01/04	30	01/04	31
May	01/05	28	02/05	30
June	29/05	27	02/06	29
July	26/06	27	01/07	29
August	23/07	27	30/07	28
September	20/08	29	28/08	29
October	19/09	30	27/09	29
November	19/10	32	26/10	30
December	21/11	33	26/11	31

The dates are referred to the present-day calendar with 30-day months.

Acknowledgments. We particularly thank K. E. Taylor for many controversial but very stimulating discussions about insolation. We also acknowledge A. Berger and M. F. Loutre for helpful comments on astronomical seasons. We thank N. de Noblet and G. Ramstein for their participation in the model simulations as well as J. Y. Peterschmitt for his useful improvement of the graphic package. We thank the Laboratoire de Météorologie Dynamique for providing us their AGCM. This work was supported by an EEC contract EV5V-CT94-0457 and computing time provided by the Commissariat à l'Energie Atomique.

References

Berger, A., Long-term variations of daily insolation and Quaternary climatic changes, *J. Atmos. Sci.*, *35*, 2362–2367, 1978.

Berger, A., Milankovitch theory and climate, *Rev. Geophys.*, *26*, 624–657, 1988.

Berger, A., and M. F. Loutre, Insolation values for the climate of the last 10 million years, *Quat. Sci. Rev.*, *10*(4), 297–317, 1991.

Berger, A., and M. F. Loutre, Precession, eccentricity, obliquity, insolation and paleoclimates, *NATO ASI Ser., Long-Term Climatic Variations*, *I*(22), 107–145, 1994.

de Noblet N., P. Braconnot, S. Joussaume, and V. Masson, Sensitivity of summer monsoon regimes to orbitally induced variations in insolation 126000, 115000 and 6000 years before present, *Clim. Dyn.*, *12*, 598–603, 1996.

Fouquart, Y., and B. Bonnel, Computations of solar heating of the Earth's atmosphere: A new parameterization, *Beitr. Phys. Atmos.*, *53*, 35–62, 1980.

Gallimore, R. G., and J. E. Kutzbach, Snow cover and sea ice sensitivity to generic changes in Earth orbital parameters, *J. Geophys. Res.*, *100*, 1103–1130, 1995.

Imbrie, J., et al., On the structure and origin of major glaciation cycles, 1, Linear responses to Milankovitch Forcing, *Paleoceanography*, *7*, 701–738, 1992.

Joussaume, S., and K. Taylor, Status of the paleoclimate modeling intercomparison project (PMIP), in *Proceedings of the First International AMIP Scientific Conference*, *WCRP-92*, *WMO/TD-732*, pp. 425–430, World Meteorol. Organ., Geneva, 1995.

Kuo, H. L., On the formation and intensification of tropical cyclones through latent heat release by cumulus convection, *J. Atmos. Sci.*, *22*, 40–63, 1965.

Kutzbach, J. E., and R. G. Gallimore, Sensitivity of a coupled atmosphere/mixed layer ocean model to changes in orbital forcing at 9000 years B.P., *J. Geophys. Res.*, *93*, 803–821, 1988.

Kutzbach, J. E., and B. L. Otto-Bliesner, The sensitivity of the African-Asian monsoon climate to orbital parameter changes for 9000 years B.P. in a low-resolution general circulation model, *J. Atmos. Sci.*, *39*, 1177–1188, 1982.

Kutzbach, J. E., and F. A. Street-Perrot, Milankovitch forcing of fluctuations in the level of tropical lakes from 18 to 0 kyr BP, *Nature*, *317*, 130–134, 1985.

Laskar, J., F. Joutel, and F. Boudin, Orbital, precessional, and insolation quantities for the Earth from −20 Myr to +10 Myr, *Astron. Astrophys.*, *270*, 522–533, 1993.

Laval, K., R. Sadourny, and V. Serafini, Land surface processes in a simplified GCM, *Geophys. Astrophys. Fluid Dyn.*, *17*, 129–150, 1981.

Le Treut, H., and K. Laval, The importance of cloud-radiation interaction for the simulation of climate, in *New Perspectives in Climate Modelling*, edited by A. Berger and C. Nicolis, *Dev. in Atmos. Sci.*, *16*, 199–221, 1984.

Le Treut, H., and Z. X. Li, Sensitivity of an atmospheric general circulation model to prescribed SST changes: Feedback effect associated with the simulation of the cloud optical properties, *Clim. Dyn.*, *5*, 175–187, 1991.

Manabe, S., and R. F. Strickleer, Thermal equilibrium in the atmosphere with a convective adjustment, *J. Atmos. Sci.*, *21*, 361–385, 1964.

Milankovitch, M., Théorie mathématique des phénomènes thermiques produits par la radiation solaire, Gauthier-Villars, Paris, 1920.

Loutre, M. F., Paramètres orbitaux et cycles diurnes et saisonniers des insolations, Ph.D. thesis, Fac. des Sci., Univ. Cath. de Louvain, Louvain-la-Neuve, France, 1993.

Mitchell, J. F. B., N. S. Grahame, and N. K. J., Climate simulations for 9000 years before present: Seasonal variations and effects of the Laurentide ice sheet, *J. Geophys. Res.*, *93*, 8283–8303, 1988.

Morcrette, J. J., Radiation and cloud radiative properties in the ECMWF operational weather forecast model, *J. Geophys. Res.*, *96*, 9121–9132, 1991.

Phillipps, P. J., and I. M. Held, The response to orbital perturbations in an atmospheric model coupled to a slab ocean, *J. Clim.*, *7*, 767–782, 1994.

Rind, D., D. Pettet, and G. Kukla, Can Milankovitch orbital variations initiate the growth of ice sheets in a general circulation model?, *J. Geophys. Res.*, *94*, 12,851–12,871, 1989.

Royer, J. F., M. Déqué, and P. Pestiaux, A sensitivity experiment to astronomical forcing with a spectral GCM: Simulation of the annual cycle at 125 000 and 115 000 BP, in *Milankovitch and Climate*, part 2, edited by A. L. Berger et al., pp. 733–763, 1984.

Sadourny, R., and K. Laval, January and July performance of the LMD general circulation model, *New Perspectives in Climate Modelling*, edited by A. Berger and C. Nicolis, *Dev. in Atmos. Sci.*, *16*, 173–198, 1984.

Schutz, C., and W. L. Gates, Global climatic data for surface, 800 mb, 400 mb, *Tech. Rep. 1029*, Rand Corp., ARPA, Santa Monica, Calif., 1972.

Slingo, A., Insolation calculation for a 360-day year, *Meteorol. O 20 Tech. Note*, Meteorol. Office, Bracknell, England, 1982.

Suarez, M. J., and I. M. Held, The sensitivity of an energy balance climate model to variations in the orbital parameters, *J. Geophys. Res.*, *84*, 4825–4836, 1979.

P. Braconnot and S. Joussaume, LMCE, DSM, Orme des Merisiers, Bât 709, CE Saclay, 91191 Gif-sur-Yvette, Cedex France. (e-mail: syljous@lmce.saclay.cea.fr)

(Received September 2, 1995; revised May 10, 1996;
accepted May 30, 1996.)